Eur. Phys. J. D **28**, 59–66 (2004)
DOI: 10.1140/epjd/e2003-00289-y

THE EUROPEAN PHYSICAL JOURNAL D

Diode laser based detection and determination of pressure-induced broadening coefficients in the $\nu_1 + \nu_3$ combination band of ammonia

J.S. Gibb, G. Hancock[a], R. Peverall, G.A.D Ritchie, and L.J. Russell

Physical and Theoretical Chemistry Laboratory, University of Oxford, South Parks Road, Oxford OX1 3QZ, UK

Received 14 March 2003 / Received in final form 13 August 2003
Published online 21 October 2003 –

Abstract. Nitrogen, oxygen, air and self-broadening coefficients have been measured in direct absorption for six transitions in the $\nu_1+\nu_3$ combination band of ammonia at room temperature using a DFB diode laser operating at 1.51 μm. Absorption cross-sections for these strong lines, suitable for detection purposes, have been determined. Using $2f$ wavelength modulation spectroscopy we demonstrate a minimum detectable concentration of 500 ppb in a 75 cm path in 1 s at atmospheric pressure and present a simple method for measurement of broadening coefficients.

PACS. 33.20.Ea Infrared spectra – 33.20.Vq Vibration-rotation analysis – 33.70.Jg Line and band widths, shapes, and shifts

1 Introduction

Both environmental monitoring and industrial applications require the sensitive and selective detection of trace gases. Ammonia is widely used in industrial processing where compact real-time detectors are employed to monitor emissions of this gas. For example, in noncatalytic NO_x reduction processes, ammonia is present in the flue gases at well below 5 ppm [1], and its concentration must be controlled to optimise consumption of the gas while reducing corrosion and environmental impact. Legislation concerning the emission of atmospheric pollutant gases has lead to the search for inexpensive methods of detection, and diode lasers have been successful in meeting this challenge [2].

In the near IR, where semiconductor diode lasers have been developed for use in the telecommunications industry, ammonia has a rich spectrum in the $\nu_1 + \nu_3$ and $2\nu_3$ bands (from $\sim$6400−6900 cm^{-1}) [3]. Regions of this spectrum free from interference from other absorbers have been identified [4], and portable diode-laser based sensors developed [1,5–10], using a variety of spectroscopic detection techniques including long-path direct absorption [5], wavelength modulation [6], optoacoustic detection [7], two-tone frequency modulation [8], cavity-enhanced absorption [9] and cavity-ringdown spectroscopy [10]. The absorptions due to ammonia in these regions of interest must be accurately quantified if they are to be applicable under a range of conditions, and this requires knowledge of the integrated absorption cross-sections and pressure broadening coefficients of the transitions.

[a] e-mail: gus.hancock@chemistry.ox.ac.uk

In this study we use direct absorption to measure integrated absorption cross-sections and pressure broadening coefficients on isolated lines in the $\nu_1 + \nu_3$ combination band of ammonia near 1.51 μm for nitrogen, oxygen, air and ammonia itself as broadening partners. Many studies have been undertaken to determine the pressure broadening coefficients for these gases in the ν_1 [11,12], ν_2 [13–16], and ν_4 [16,17] fundamental bands using both FTIR and direct absorption techniques, but there have been relatively few studies undertaken on the overtone or combination bands. Pressure broadening coefficients have been measured in the $4\nu_1$ and $2\nu_1 + 2\nu_3$ [18], and $\nu_1 + \nu_3$ bands [8,9] using direct absorption methods. Because of the weaker absorption cross-sections in these regions, compared with those of the fundamental bands, more sensitive techniques such as modulation spectroscopy (wavelength modulation or two-tone frequency modulation) [18] or cavity enhanced absorption spectroscopy [9] have been proposed for detection purposes.

Wavelength modulation spectroscopy (WMS) has greater detection sensitivity than direct absorption. In this technique, modulation of the diode laser's injection current at frequency f and subsequent nth harmonic detection gives nf signals that are qualitatively similar to the nth derivative of the absorption spectrum. Known concentrations of absorbing species may then be used to calibrate the WMS signal [19] for quantitative trace gas detection. Here we demonstrate the use of $2f$ WMS for the sensitive detection of ammonia.

Under the modulation regimes where maximum sensitivity is achieved [20] the lineshapes exhibit modulation

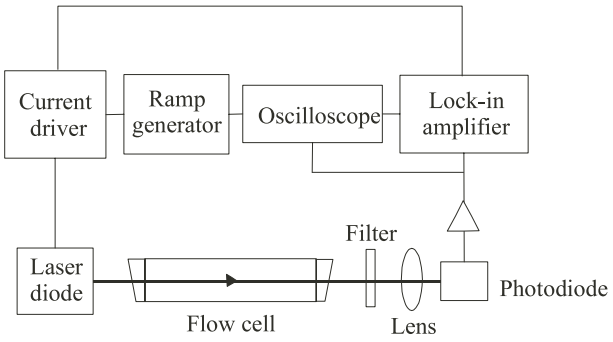

Fig. 1. Experimental arrangement. The current driver for the laser diode receives a triangular wave signal from the ramp generator, monitored on the oscilloscope, and for WMS also receives a sinusoidal signal from the internal reference of the lock-in amplifier. The signal received from the photodiode is monitored directly using the oscilloscope, or demodulated by the lock-in amplifier to give the $2f$ WMS trace.

broadening, such that integration of the observed signals recovers absorption profiles wider than the true profile. More complex analysis of the WMS lineshape is therefore required if pressure-broadening data are to be recovered. Yelleswarapu and Sharma used the variation in WMS peak height to find the self-broadening coefficients of acetylene [21], while for ammonia Lucchesini et al. fitted the entire WMS lineshape in the derivative limit [22,23]. However, the former method requires knowledge of the absorber concentration, while the latter is complex for the maximum sensitivity regimes, where the lineshape is not given by the derivative. Here we present a simple method for the determination of pressure induced broadening using $2f$ WMS which does not require prior knowledge of the ammonia concentration, provided that the concentration is sufficiently low that self-broadening may be neglected, a condition which is most easily satisfied in the high sensitivity regimes of WMS.

2 Experimental

The apparatus used for these experiments is shown in Figure 1. The 1.51 μm DFB diode laser (Bookham Technology, quoted bandwidth 1.34 MHz) is mounted on a brass block, thermally stabilised and collimated using a standard anti-reflection-coated lens. The laser operates without external feedback and can be tuned mode hop free over 6 nm using both temperature and current. For the frequencies of interest, the diode is operated in the ranges 38–45 °C and 180–220 mA, giving powers between 19 and 22 mW. Application of a triangular wave ramp voltage to the diode injection current allows the frequency to be scanned. The scanning range depends on the frequency of the ramp and peak-to-peak voltage applied (in the range 6–15 V), but is typically around 10 GHz, as observed using a spectrum analyser (Melles Griot, free spectral range 10 GHz) and confirmed by the known separation of the observed peaks [3].

The laser radiation passes through a 75 cm long cell containing the sample gases and is focussed onto an amplified photodiode (New Focus 1611-AC). For the direct absorption studies, the current is ramped at 12 Hz and the signal averaged over 100 scans. For the WMS studies, the current is ramped at 8 mHz while simultaneously being modulated by a 10 kHz sine wave from the internal reference of a lock-in amplifier (Perkin Elmer 7265). The signal from the photodiode is demodulated at twice the modulation frequency to give the $2f$ signal. The effect of the sinusoidal modulation is observed using the spectrum analyser and is found to give a modulation amplitude of 0.8–0.85 GHz, depending on the frequency region scanned by the laser. This value is confirmed by the observed width of a $2f$ WMS signal from the Gaussian absorption due to a low pressure ammonia sample. Ammonia is introduced at pressures of a few hundred mTorr, and the pressure allowed to stabilise over 30 minutes. The initial pressure is seen to fall over this time, as ammonia is adsorbed onto the cell walls. The first measurement is then recorded and the broadening gas added. Ten minutes were allowed between each measurement to ensure pressure stability for foreign gas broadening, and twenty minutes for self-broadening. All experiments were carried out at room temperature (295 K).

3 Results and analysis

Three regions (A–C: see Fig. 2) of the ammonia absorption spectrum accessible with our DFB laser have been considered, each containing a pair of strong lines: (A1) at 6600.182 cm^{-1} and (A2) at 6599.893 cm^{-1}, (B1) at 6595.923 cm^{-1}and (B2) at 6595.616 cm^{-1}, (C1) at 6595.241 cm^{-1} and (C2) at 6595.063 cm^{-1} [3]. These correspond to some of the strongest absorption cross-sections in this spectral region. Regions (A) and (B) are free from water absorption lines, while (C) contains only very weak water absorption features [24]. Lines (A1) and (A2) are unassigned, but they lie in what has been identified as a useful region for emissions monitoring [4]. The remaining 4 lines have been assigned by Lundsberg-Nielsen et al. [3] as (B1) = ${}^{R}Q(4,1)$ (a), (B2) = ${}^{Q}P(10,6)$ (s), (C1) = ${}^{R}Q(5,1)$ (s) and (C2) = ${}^{R}Q(5,1)$ (a) respectively, where the notation gives ${}^{\Delta K}\Delta J(J'',K'')$ and (s) and (a) correspond to symmetric and asymmetric inversion symmetry for the $\nu_1+\nu_3$ rovibrational band. Wavenumbers and assignments are given in Table 1.

3.1 Direct absorption

Figure 2 shows the low pressure profiles observed in direct absorption for the three regions, (A–C). The six strong lines listed in Table 1 are readily identified: the weaker features in regions (A) and (B) are caused by ammonia absorption, but remain unassigned. The background intensity variation of the diode laser output has been removed by fitting to a polynomial and the frequency calibration was obtained from the separation of the known lines.

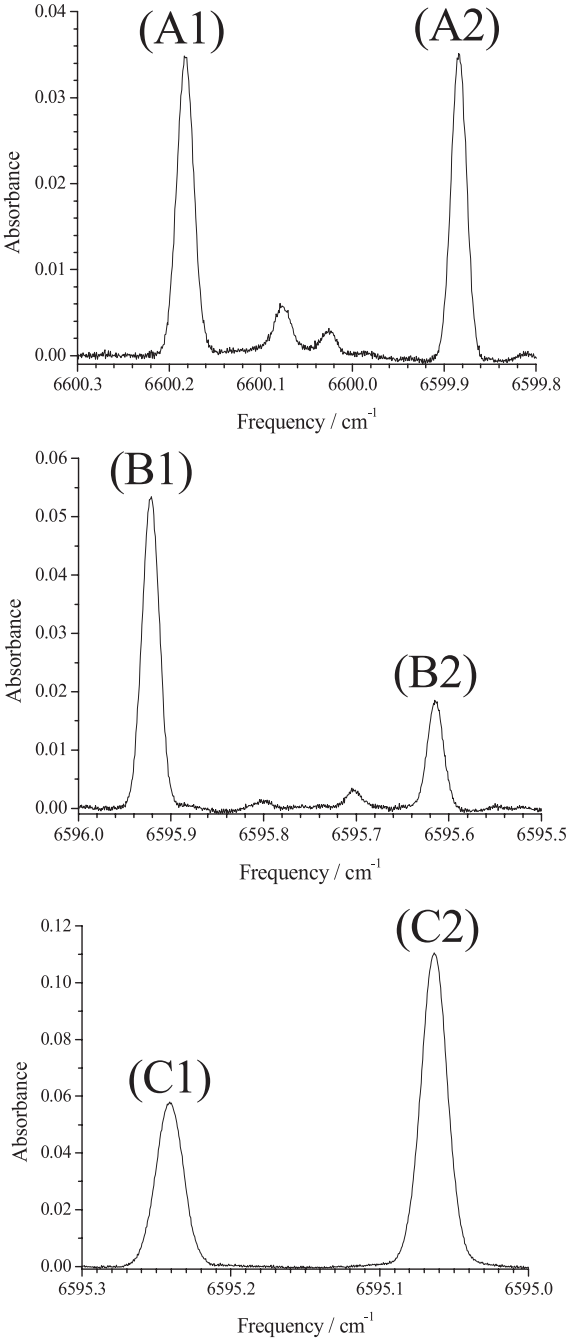

Fig. 2. Direct absorption traces for pure ammonia at pressures of 215, 820 and 612 mTorr for regions (A) upper panel, (B) middle panel and (C) lower panel, respectively, in the 75 cm single pass cell. Assigned lines are listed in Table 1.

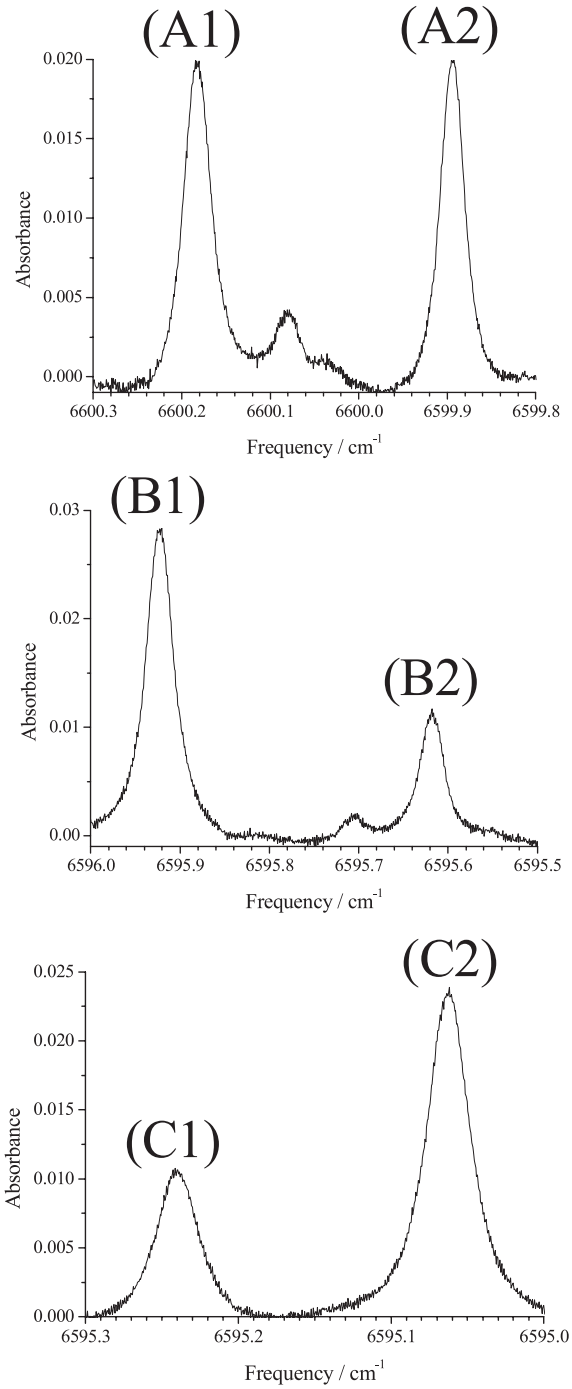

Fig. 3. Direct absorption traces as in Figure 2 but with 100 Torr added N_2.

The traces were fitted well by Gaussian profiles of 295 MHz half-width half-maximum (HWHM), in keeping with a room temperature (295 K) Doppler broadened sample. Integrated absorption cross-sections were obtained from a plot of integrated absorbance versus pressure for a series of direct absorption traces in pure ammonia and are shown in Table 1. These may be compared with those previously determined using an FTIR spectrometer by Lundsberg-Nielsen et al. [3] and in diode laser studies by Webber et al. [4].

Examples of pressure broadened traces, in this case with 100 Torr of nitrogen present, are shown in Figure 3, again with the background removed. These were fitted using a Voigt profile, with the Gaussian width fixed to that

Table 1. Integrated absorption cross-sections for the six ammonia lines together with their wavenumbers and assignments (for notation see Sect. 3). Errors are estimated from the fit to the plots of integrated absorbance against pressure, the error in the sample length and potential systematic error in the pressure. The results are compared with previous measurements quoted in references [3,4] as explained in the text.

			Integrated absorption cross-section / 10^{-22} cm^2 cm^{-1}		
Line	Frequency / cm^{-1}	Assignments	Our results	Ref. [3]	Ref. [4]
A1	6600.182	—	11.98 ± 0.67	11.58 ± 0.08	12.50 ± 0.38
A2	6599.893	—	12.92 ± 0.72	12.20 ± 0.08	13.31 ± 0.40
B1	6595.923	$^{R}Q(4,1)$ (a)	6.35 ± 0.35	6.36 ± 0.07	—
B2	6595.616	$^{Q}P(10,6)$ (s)	2.14 ± 0.12	2.07 ± 0.06	—
C1	6595.241	$^{R}Q(5,1)$ (s)	3.32 ± 0.18	3.35 ± 0.06	—
C2	6595.063	$^{R}Q(5,1)$ (a)	6.52 ± 0.35	6.25 ± 0.06	—

observed at low pressures:

$$\delta(\nu, w_L) = A\int_{-\infty}^{\infty} \frac{e^{-t^2}}{\left(\sqrt{\ln 2}\frac{w_L}{w_G}\right)^2 + \left(\sqrt{\ln 2}\left(\frac{\nu-\nu_C}{w_G}\right) - t\right)^2}\, dt \quad (1)$$

where w_G, w_L are the Gaussian and Lorentzian HWHM, A is a constant, ν is the frequency, and ν_C is the line-centre frequency. Where the scan shows another ammonia absorption that begins to overlap with the absorption feature of interest, such as in scans (A) and (B), the Voigt fitted was weighted away from this region. Using a Galatry function to fit the direct absorption data did not improve the quality of the fit, indicating that Dicke narrowing is not significant for our studies [25].

For pure ammonia the returned Lorentzian width was found to be a linear function of pressure, and was measured in the range up to 15 Torr. For the gas mixtures, the Lorentzian component was first corrected for broadening by ammonia, the effect of which was largest at the smallest added gas pressure, and was typically of the order of 10 MHz. The resultant broadening was again found to be proportional to the pressure of added gas, and a plot of the returned Lorentzian HWHM against pressure gives a straight line with gradient γ, the pressure broadening coefficient. An example of the plots obtained in this way is shown in Figure 4 for the strongest absorption line, (A2) at 6599.893 cm^{-1}, and the values of γ are given in Table 2. The errors on the individual points for the direct absorption data in Figure 4 are a combination of those from the Voigt fit and an estimate of the reproducibility of the data (the dominant effect) and are seen to be small. Overall errors in γ are calculated by combining these with a possible systematic error in the pressure reading (taken to be 5%).

3.2 Wavelength modulation

In WMS, modulation of the diode laser injection current results in an instantaneous laser frequency given by:

$$\nu(t) = \nu_0 + W\sin(2\pi\nu_m t) \quad (2)$$

where ν_0 is the carrier optical frequency (the unperturbed laser frequency), W is the modulation amplitude of the laser frequency and ν_m is the modulation frequency (here 10 kHz). The laser frequency, ν_0, is ramped across the absorption lines whilst being simultaneously modulated at frequency ν_m. The harmonic component at twice the modulation frequency, which is measured by the photodetector and subsequently demodulated by the lock-in amplifier, is given by:

$$K_2(\nu, w_L) = B\int_0^{\pi} \delta(\nu + W\cos\theta, w_L)\cos 2\theta\, d\theta \quad (3)$$

where B is a constant and $\delta(\nu, w_L)$ is the absorbance of the sample. This expression assumes that there is no variation in intensity of the incident light, which can be a problem in some WMS experiments [22]. However, in our case, over 1.7 GHz (corresponding to $2W$, the maximum excursion of the laser frequency for a given ν_0), the variation in incident intensity is less than 1.5%, and this approximation is valid. Weak absorption is also assumed with $\delta(\nu, w_L) \ll 1$. Typical examples of the observed $2f$ WMS traces for a low pressure ammonia sample are given in Figure 5.

For the WMS studies, W is chosen to be more than twice the expected HWHM in order to maximise the detection sensitivity [20]. The bandwidth reduced minimum detectable absorption due to ammonia at 6595.923 cm^{-1} is 3.6×10^{-5} Hz$^{-1/2}$ in direct absorption, while using WMS improves this value to 1.0×10^{-5} Hz$^{-1/2}$. We attribute the high comparable sensitivity of the direct absorption measurement to the intrinsic stability of the DFB diode laser, and note that the relative improvement in sensitivity afforded by WMS would be greater under detection conditions where there are higher levels of low frequency noise, or at higher modulation frequencies.

The choice of W to maximise sensitivity also means that the observed traces are significantly broadened by the modulation. Clearly, measurements taken directly from the integrated lineshape would overestimate the width and lead to systematic errors in the pressure broadening coefficients. In order to use WMS in pressure broadening studies, it is necessary to understand how the modulation broadened lineshape changes as the absorption is pressure

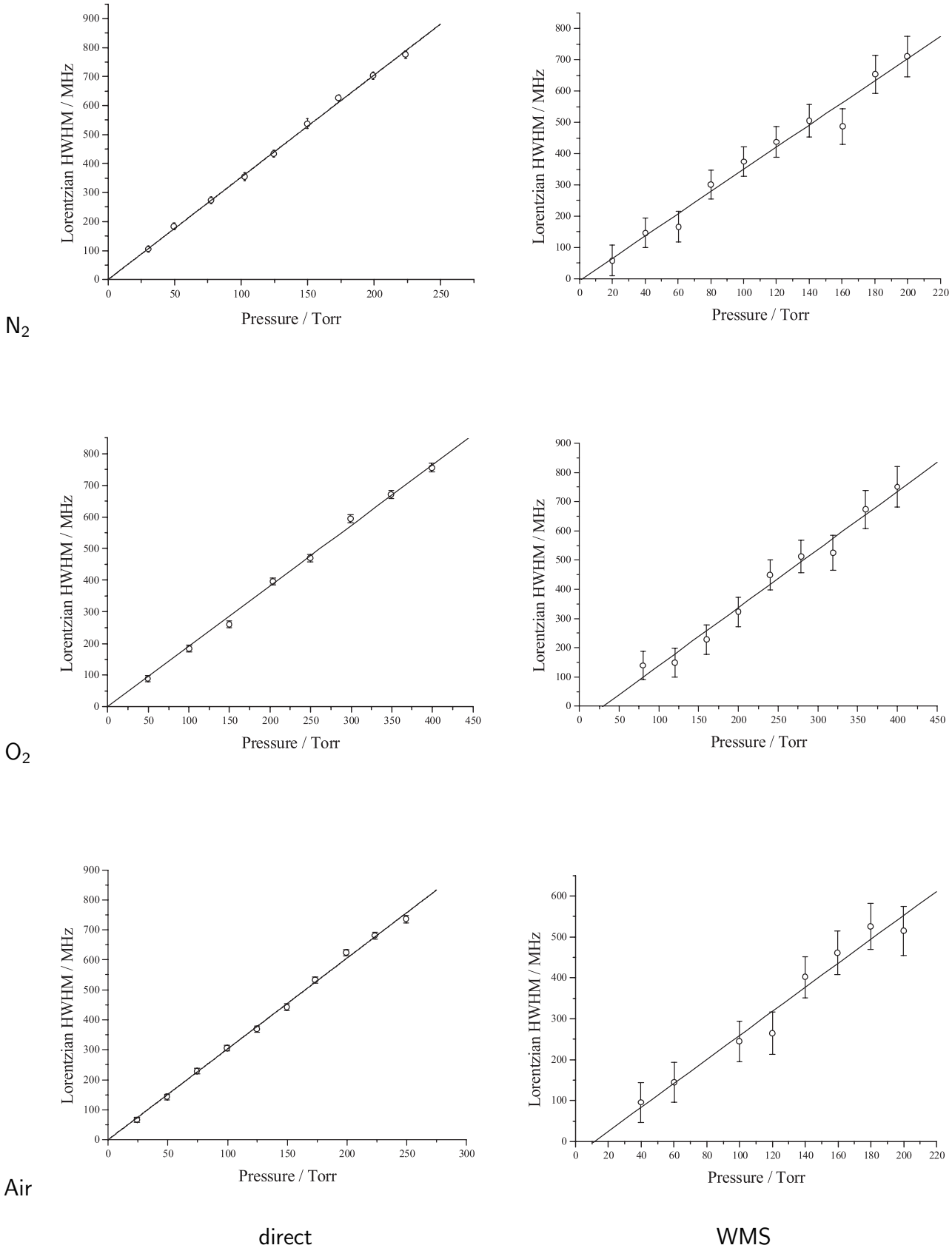

Fig. 4. Plots of Lorentzian component (HWHM) of the pressure broadening for the (A2) line of ammonia at 6599.893 cm^{-1} as a function of added N_2, O_2 and air. The left hand figures show the direct measurements, the right hand figures are for WMS. Error bars are calculated as explained in the text. The slope of the lines yields the broadening coefficients γ listed in Table 2.

Table 2. Pressure induced broadening coefficients γ for the six absorption features found by using direct absorption and WMS, all referring to HWHM values. The differences between direct and WMS values are also given as a percentage of the direct values. Errors are calculated as explained in the text.

Line	Frequency (cm^{-1})	Direct	WMS	Difference (%)
		$\gamma(N_2)$ / MHz $Torr^{-1}$		
A1	6600.182	3.56 ± 0.18	3.54 ± 0.38	−0.7
A2	6599.893	3.53 ± 0.18	3.47 ± 0.38	−1.6
B1	6595.923	3.63 ± 0.19	3.65 ± 0.69	+0.5
B2	6595.616	2.74 ± 0.15	2.33 ± 0.65	−14.9
C1	6595.241	2.97 ± 0.16	3.20 ± 0.39	+7.7
C2	6595.063	3.39 ± 0.18	3.26 ± 0.43	−3.8
		$\gamma(O_2)$ / MHz $Torr^{-1}$		
A1	6600.182	2.09 ± 0.11	2.16 ± 0.20	+3.1
A2	6599.893	1.91 ± 0.10	2.07 ± 0.20	+8.3
B1	6595.923	1.93 ± 0.10	2.18 ± 0.20	+13.0
B2	6595.616	1.48 ± 0.10	1.74 ± 0.18	+17.8
C1	6595.241	1.73 ± 0.08	1.97 ± 0.19	+13.9
C2	6595.063	1.69 ± 0.09	2.00 ± 0.20	+18.2
		γ(air) / MHz $Torr^{-1}$		
A1	6600.182	3.14 ± 0.17	3.41 ± 0.41	+8.5
A2	6599.893	3.04 ± 0.16	2.93 ± 0.39	−3.6
B1	6595.923	3.22 ± 0.17	3.48 ± 0.42	+8.1
B2	6595.616	2.46 ± 0.14	3.05 ± 0.40	+23.9
C1	6595.241	2.90 ± 0.15	3.09 ± 0.33	+6.6
C2	6595.063	2.81 ± 0.15	2.99 ± 0.40	+6.6
		$\gamma(NH_3)$ / MHz $Torr^{-1}$		
A1	6600.182	23.56 ± 1.23		
A2	6599.893	23.11 ± 1.21		
B1	6595.923	15.67 ± 0.86		
B2	6595.616	11.27 ± 0.69		
C1	6595.241	10.99 ± 0.69		
C2	6595.063	12.58 ± 0.75		

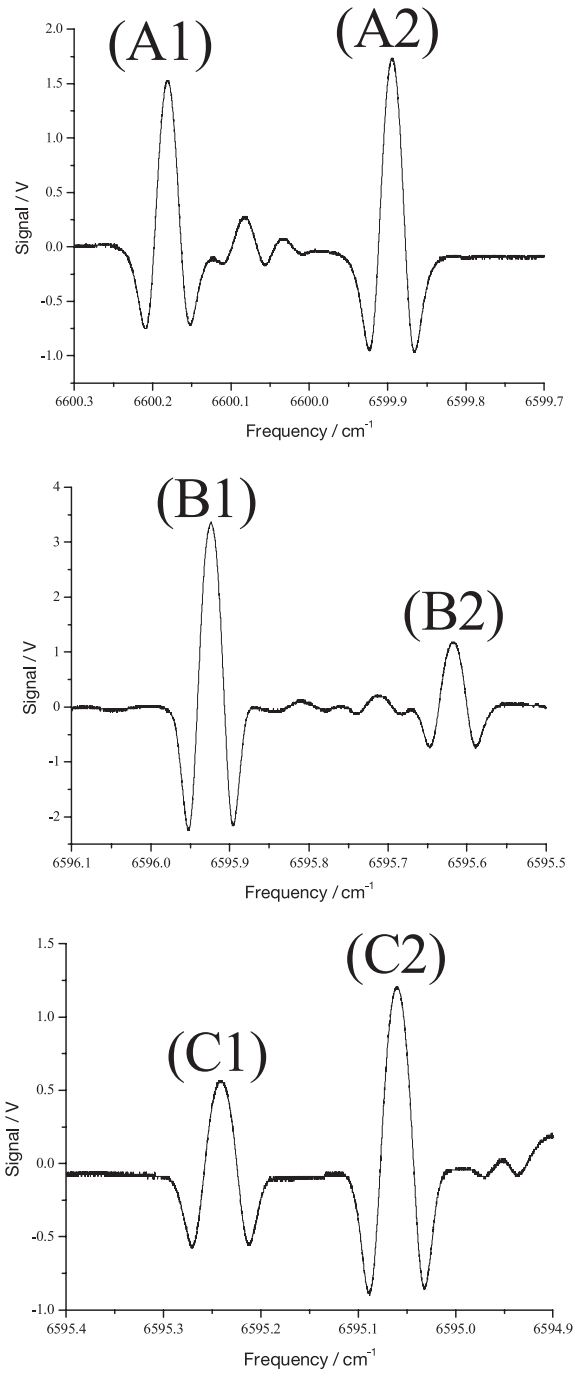

Fig. 5. $2f$ WMS traces in regions (A–C) for pure ammonia present at pressures of 100, 700 and 300 mTorr respectively.

broadened. Where the concentration of the absorber is known, the variation of peak height of the $2f$ WMS signal with pressure may be used to determine γ [21]. However, where the concentration of the absorber is not accurately known, as may well be the case in studies where the concentration is too low to allow direct absorption to be used as a calibrant, a consideration of the whole lineshape becomes necessary in order to extract values of γ.

The approximate method we propose here has the advantage that it neither requires the concentration of the absorbing species to be known, provided that it is sufficiently small for self-broadening to be negligible, nor requires a fit to the whole WMS lineshape in order to determine pressure-broadening coefficients. It relies on a calibration curve relating the peak-to-peak separation Δ of the outer turning points of the $2f$ WMS lineshape to the width of the Lorentzian component of the broadened line, and is similar to the method proposed by Minguzzi and DiLieto for the analysis of Voigt profiles [26]. Figure 6 illustrates the definition of Δ and shows the calibration curve calculated from WMS profiles given by equation (3) for a single isolated ammonia absorption feature with a Doppler width appropriate to 295 K and with our experimentally determined value of $W = 850$ MHz.

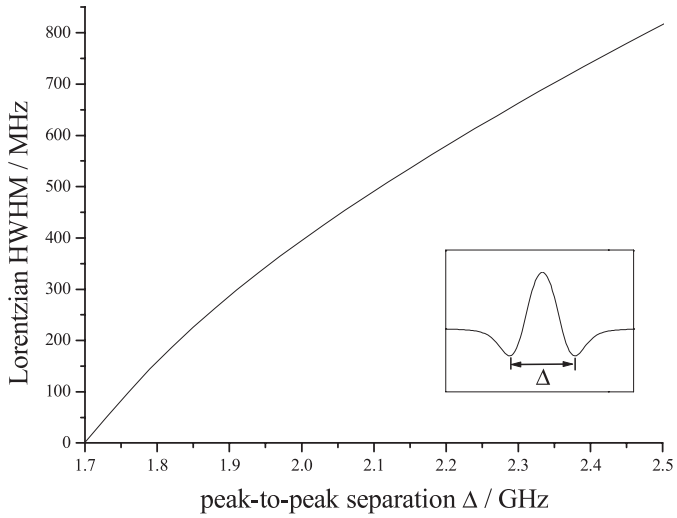

Fig. 6. Calibration curve relating the calculated separation Δ of the outer turning points of the $2f$ WMS trace to the Lorentzian HWHM of the added gas broadening for an ammonia transition at 295 K. The inset shows the definition of Δ.

This calibration curve is used to convert the values of Δ measured from the experimental $2f$ traces to the corresponding Lorentzian HWHM resulting from added gas broadening. The Lorentzian contributions are then plotted against pressure as for the direct studies. Examples of this are shown in Figure 4, and the resulting γ given in Table 2.

The errors on the individual points are those estimated in the measurement of Δ from the observed traces, and are propagated through equation (3) and the calibration curve (Fig. 6): these errors could be reduced by a complete line fitting procedure, but this is not the purpose of this study — instead we are interested if this simple measurement procedure is able to determine values of γ. We note that larger errors will be introduced at low pressures, where modulation broadening is a significant contributor to the observed linewidth. The total error in γ includes the statistical error from the least squares fit, an estimate of the error caused by a 50 MHz uncertainty in W and possible systematic error in the pressure (taken to be 5% as before). The physically unreasonable small negative intercepts in some of the WMS data of Figure 4 reflect these sources of error. Nevertheless it can be seen from Table 2 that with the exception of the (B2) feature at 6595.616 cm^{-1} the WMS and direct data are in good agreement for N_2 and air, and WMS are on average some 12% higher for added O_2.

Within regions (A) and (B) there are other ammonia peaks with lower absorption cross-sections and the lineshapes due to these features are seen to broaden and overlap with the absorptions under study. In general direct broadening measurements were made under conditions where this effect was minimal or could be allowed for. Moving to nth harmonic WMS detection allows the different absorption lines to be more clearly seen because of the increased number of turning points seen in the spectra with increasing n [27]. However, the sensitivity of the peak-to-peak separation of the WMS lineshape for each individual absorption line to the Lorentzian HWHM decreases with n. As a result, $2f$ WMS proves to be the most appropriate technique for our measurements, allowing some resolution of overlapping lineshapes in (A) and (B), while still being sensitive to the increase in Lorentzian width. It should be noted however that the largest discrepancy between direct and WMS measurements occurs for line (B2) at 6595.616 cm^{-1} where the effect of overlap is largest: for the more isolated and strongest absorbing line (A2) at 6599.893 cm^{-1} the two techniques are in very good agreement. We conclude that the simple WMS method of obtaining values of γ will yield acceptable results providing there is no marked influence from neighbouring features, and could be of value where direct measurements are too insensitive.

4 Discussion of the results

The integrated absorption cross-sections for 6 absorption lines of ammonia around 1.51 μm have been measured. In order to allow comparison with previous peak cross-sections found by Lundsberg-Nielsen et al. [3] the latter results were converted into an integrated absorption cross-section, using our self-broadening coefficients. It can be seen that our values are in good agreement with both those found in [3] for all 6 lines and those for lines (A1) and (A2) reported by Webber et al. [4].

The values obtained for the pressure broadening coefficients γ can be compared to the measurements previously taken in this band [8,9], and to those of similar transitions in the ν_1 fundamental [11], $4\nu_1$ overtone and $2\nu_1+2\nu_3$ combination band [18,23]. In the fundamental band, similar values for γ_{N_2} and γ_{O_2} of around 4 and 2 MHz $Torr^{-1}$ have been found respectively. The γ_{NH_3} values in this band are in the region of 16–25 MHz $Torr^{-1}$, somewhat larger than those returned for our assigned lines, though comparable with those for the unassigned pair, (A). In the $2\nu_1 + 2\nu_3$ combination band [18], γ_{NH_3} were found to be in the region 11–13 MHz $Torr^{-1}$, while γ_{air} was around 5 MHz $Torr^{-1}$. For the ten transitions studied by Lucchesini and Gozzini around 790 nm [23], belonging to the $4\nu_3$ and $2\nu_1+2\nu_3$ bands, γ_{air} was found to be in the region 3.2–4.2 MHz $Torr^{-1}$ and γ_{NH_3} 11.4–23.1 MHz $Torr^{-1}$. The large range of self-broadening parameters is consistent with that found in our study. In the $\nu_1 + \nu_3$ band, where our absorptions lie, Modugno et al. [8] found $\gamma_{N_2} = 3.32$ MHz $Torr^{-1}$ and $\gamma_{NH_3} = 19.7$ MHz $Torr^{-1}$ for ${}^{P}P(7,3)$ (s) and $\gamma_{N_2} = 3.10$ MHz $Torr^{-1}$ and $\gamma_{NH_3} = 20.5$ MHz $Torr^{-1}$ for ${}^{R}P(6,0)$ (a), while Peeters et al. [9] found $\gamma_{air} = 3$ MHz $Torr^{-1}$ and $\gamma_{NH_3} = 10$ MHz $Torr^{-1}$ for the ${}^{R}R(0,0)$ (a) transition. The values are within the range of the present measurements.

The predominant collisional interaction that leads to broadening of the absorption lineshape by oxygen and nitrogen may be assumed to be dipole-quadrupole in character. The higher value of γ_{N_2} compared to γ_{O_2} is caused by the larger quadrupole moment of nitrogen compared to

oxygen as expected. Calculated average values of γ over the Boltzmann distribution of the four observed and identified energy levels yields a ratio of γ_{N_2} to γ_{O_2} of 1.9 for the direct measurements, which compares well with similar studies on H_2O [28], HCl, HF [29] and OH [30] by other workers, where this value is in the region of 1.7. We note that capture theory based purely on electrostatic interactions as employed by Hofzumahaus and Stuhl [31] predicts a ratio of 1.25. The air pressure induced broadening coefficients may be predicted from an average of the oxygen and nitrogen values, weighted according to their relative atmospheric abundance: $\gamma_{air} = 0.79\gamma_{N_2} + 0.21\gamma_{O_2}$. No significant difference is seen between the predicted and measured values, indicating that the effects of O_2 and N_2 appear to be additive. For self-broadening, the main interaction is dipole-dipole, and is therefore stronger and longer range. This results in larger pressure broadening coefficients than for the foreign perturbers. There is also an extra contribution to the self-broadening from resonant energy exchange between colliding NH_3 molecules.

We finally comment on the sensitivity of WMS in this experiment. For the strongest and uncongested transition, (A2) at 6599.893 cm^{-1}, the observed WMS signal was first calibrated at higher ammonia pressures against direct absorption, and the resultant signal to noise ratio indicated that a minimum detectable concentration of ammonia in an air broadened sample at atmospheric pressure is 500 ppb for a 1 s observation time. This corresponds to a fractional absorption of 1.25×10^{-7} cm^{-1}. For a typical cavity-enhanced absorption spectroscopy experiment [9] with a minimum detectable fractional absorption of the order of 1×10^{-8} cm^{-1}, this same transition would give a minimum detectable concentration of 40 ppb in 1 s at atmospheric pressure.

5 Conclusions

Integrated absorption cross-sections and pressure broadening coefficients are reported for six lines in the $\nu_1 + \nu_3$ combination band of ammonia, measured both in direct absorption and wavelength modulation spectroscopy. The effect of modulation broadening on the observed $2f$ WMS spectra has been quantified, and calibration curves for the modulation amplitudes have been applied to return the Lorentzian widths. While WMS used in the high modulation amplitude regime gives a greater detectivity, once calibrated, than the direct absorption studies, it can be seen that it provides a less precise method for the determination of the pressure broadening coefficients: higher precision can be obtained by WMS when the modulation amplitude is much less than the linewidth (the derivative limit) at the expense of sensitivity. However, it can also be applied to weaker cross-section absorptions and allows overlapping lineshapes to be easily distinguished. If the ammonia absorptions described here are to be used for sensitive trace gas detection, then the application of WMS is an advantage.

We are grateful to the Royal Society of Chemistry and EPSRC for support of this work, and to Bookham for provision of the DFB laser under the JREI program. We thank the Ramsay Fellowship trust (GADR) and the Leverhulme Trust (RP) for postdoctoral support.

References

1. I. Linnerud, P. Kaspersen, T. Jaeger, Appl. Phys. B **67**, 297 (1998)
2. P.A. Martin, Chem. Soc. Rev. **31**, 201 (2002)
3. L. Lundsberg-Nielsen, F. Hegelund, F.M. Nicolaisen, J. Mol. Spec. **162**, 230 (1993)
4. M.E. Webber, D.S. Baer, R.K. Hanson, Appl. Opt. **40**, 2031 (2001)
5. R. Claps, F.V. Englich, D.P. Leleux, D. Richter, F.K. Tittel, R.F. Curl, Appl. Opt. **40**, 4387 (2001)
6. M. Fehér, P.A. Martin, A. Rohrbacher, A.M. Soliva, J.P. Maier, Appl. Opt. **32**, 2028 (1993)
7. A. Miklós, M. Fehér, Infrared Phys. Technol. **37**, 21 (1996)
8. G. Modugno, C. Corsi, Infrared Phys. Technol. **40**, 93 (1999)
9. R. Peeters, G. Berden, A. Apituley, G. Meijer, App. Phys. B **71**, 231 (2000)
10. A.R. Awtry, J.H. Miller, Appl. Phys. B **75**, 255 (2002)
11. A.S. Pine, V.N. Markov, G. Buffa, O. Tarrini, J. Quant. Spec. Rad. Trans. **50**, 337 (1993)
12. V.N. Markov, A.S. Pine, G. Buffa, O. Tarrini, J. Quant. Spec. Rad. Trans. **50**, 167 (1993)
13. V.S. Letokhov, A.G. Platova, O.A. Tumanov, Opt. Spectrosc. **37**, 29 (1974)
14. M. Fabian, R. Schieder, K.M.T. Yamada, G. Winnewiser, J. Mol. Spec. **177**, 294 (1996)
15. G. Baldacchini, A. Bizzarri, L. Nencici, V. Sorge, J. Quant. Spec. Rad. Trans. **43**, 371 (1990)
16. G. Baldacchini, G. Buffa, O. Tarrini, Nuovo Cim. **13**, 719 (1991)
17. H. Aroui, M. Broquier, A. Picard-Bersellini, J.P. Bouanich, M. Chevalier, S. Gherissi, J. Quant. Spec. Rad. Trans. **60** 1011 (1998)
18. A. Lucchesini, D. Pelliccia, C. Gabbanini, S. Gozzini, I. Longo, Nuovo Cim. D **16**, 117 (1994)
19. P. Werle, Spectrochim. Acta A **54**, 197 (1998)
20. J.A. Silver, Appl. Opt. **31**, 707 (1992)
21. C. Yelleswarapu, A. Sharma, J. Quant. Spectr. Rad. Trans. **72**, 733 (2002)
22. M. De Rosa, A. Ciucci, D. Pelliccia, C. Gabbanini, S. Gozzini, A. Lucchesini, Opt. Comm. **147**, 55 (1998)
23. A. Lucchesini, S. Gozzini, Eur. Phys. J. D **22**, 209 (2003)
24. HITRAN'2000 database (v 11.0)
25. P.L. Varghese, R.K. Hanson, Appl. Opt. **23**, 2376 (1984)
26. P. Minguzzi, A. DiLieto, J. Mol. Spectrosc. **109**, 388 (1985)
27. A.N. Dharamsi, A.M. Bullock, Appl. Phys. B **63**, 283 (1996)
28. B.E. Grossmann, E.V. Browell, J. Mol. Spec. **138**, 562 (1989)
29. A.S. Pine, J.P. Looney, J. Mol. Spec. **122**, 41 (1987)
30. A. Schiffman, D.J. Nesbitt, J. Chem. Phys. **100**, 2677 (1994)
31. A. Hofzumahaus, F. Stuhl, J. Chem. Phys. **82**, 3152 (1985)